9794 *Biochemistry* **2009,** *48,* 9794–9800
DOI: 10.1021/bi901102h

BIOCHEMISTRY
including biophysical chemistry & molecular biology
Article

Biochemical Characterization of the Multidrug Regulator QacR Distinguishes Residues That Are Crucial to Multidrug Binding and Induction of *qacA* Transcription[†]

Kate M. Peters,[‡] George Sharbeen,[‡] Torsten Theis,[‡] Ronald A. Skurray,[‡] and Melissa H. Brown*[,‡,§]

[‡]*School of Biological Sciences, A12, University of Sydney, Sydney, NSW, Australia, and* [§]*School of Biological Sciences, Flinders University, Adelaide, SA, Australia*

Received June 30, 2009; Revised Manuscript Received September 17, 2009

ABSTRACT: *Staphylococcus aureus* transcription factor QacR regulates expression of the *qacA* multidrug efflux determinant. In response to binding cationic lipophilic compounds, including ethidium and rhodamine 6G, QacR dissociates from the *qacA* operator alleviating repression. Such ligand binding uniformly induces a coil-to-helix transition of residues Thr^{89}−Tyr^{93} revealing an asymmetric binding pocket in QacR containing two distinct subpockets. Here, the functional significance of hydrophobic, aromatic, and polar residues characteristic of the rhodamine 6G pocket and the proximal Tyr^{92}, proposed to facilitate the transcriptionally active conformation, was examined. Notably, the presence of Tyr^{92} was not essential for QacR structural changes between DNA-bound and induced conformations. Furthermore, although mutation of the majority of residues contacting rhodamine 6G exerted moderate effects on QacR−rhodamine 6G binding, mutation of Leu^{54} and Gln^{96}, and cumulative mutations involving these with Tyr^{93} and Tyr^{123}, imparted a dramatic decrease in QacR−rhodamine 6G binding affinity. This equated with impaired dissociation of QacR from its operator DNA in the presence of this ligand in *S. aureus*, delineating the important role of these residues in the QacR−rhodamine 6G interaction. Additionally, despite maintaining a high affinity for ethidium, QacR mutants involving Leu^{54}, Tyr^{93}, Gln^{96}, and Tyr^{123}, which denote the interface between the rhodamine 6G and ethidium subpockets, were unable to be induced from operator DNA in the presence of ethidium in *S. aureus*. This highlights the significant contribution of these residues to QacR-mediated derepression of *qacA* transcription following ligand binding in the distal subpocket and may be important for the general mechanism irrespective of the ligand bound.

Multidrug resistant bacteria represent a serious threat to human and animal health that is largely facilitated by multidrug efflux transporters (*1*, *2*). These transport proteins are capable of conferring resistance to a range of structurally and chemically dissimilar compounds, and the acquisition or upregulation of a single gene can simultaneously render the cell or organism resistant to a multitude of compounds. Only a handful of high-resolution structures of these integral membrane proteins bound to ligands are available (*3*−*5*). Subsequently, current detailed knowledge regarding the multiligand binding mechanism is predominantly based on the crystallographic analyses of soluble transcription factors QacR (*6*−*9*), BmrR (*10*−*12*), and TtgR (*13*) and more recently that of LmrR (*14*), which display substrate recognition profiles similar to those of the transporters that they regulate and have been resolved in complex with multiple drugs. However, the coinciding biochemical analysis of these proteins has been limited.

A member of the TetR family of transcriptional regulators, QacR has a unique C-terminal multidrug binding and dimerization domain and a conserved N-terminal helix−turn−helix DNA binding domain. In the absence of ligand, QacR binds as a dimer to IR1 operator DNA to repress transcription of the downstream multidrug efflux determinant, *qacA* (*15*−*19*). The remarkable ability of QacR to recognize a structural diversity of monovalent and bivalent cationic, lipophilic compounds is enabled by a voluminous multisite ligand binding pocket. Comprised of distinct and overlapping subpockets, termed the rhodamine 6G (R6G)[1] and ethidium (Et) pockets after the respective monovalent ligands first identified to be bound within these regions, the surface is lined with myriad glutamate, aromatic and nonpolar residues, and several polar residues (Figure 1) (*6*−*9*). Binding of ligand to QacR is restricted to one monomer and uniformly elicits a coil−helix transition of residues Thr^{89}−Tyr^{93}, which form the induction switch region (*6*−*9*). This transition appears to be facilitated by the expulsion of Tyr^{92}, the only Ramachandran outlier in the ligand-free conformation, to a more favorable conformation outside the hydrophobic core of the protein (*6*). Residue Tyr^{93} is similarly dislodged, and together this expands the ligand binding pocket with concomitant changes reorienting the DNA binding domains and inducing QacR from the IR1 operator site (*19*). Subsequently, this conformational coil−helix trigger appears to be pivotal for the alternation between a conformation that is conducive to binding operator DNA and repressing transcription from the *qacA* promoter sequence (P_{qacA}) and, conversely, that which is favorable to the expansion of the ligand binding pocket and substrate binding with release of QacR from the operator.

[†]This work was supported by Grant 301941 from the National Health and Medical Research Council (Australia).

*To whom correspondence should be addressed: School of Biological Sciences, GPO Box 2100, Flinders University, Adelaide, SA 5001, Australia. Telephone: +618 8201 2747. Fax: +618 8201 3015. E-mail: melissa.brown@flinders.edu.au.

[1]Abbreviations: Et, ethidium; PDB, Protein Data Bank; R6G, rhodamine 6G; wt, wild type.

 Published on Web 09/17/2009 © 2009 American Chemical Society

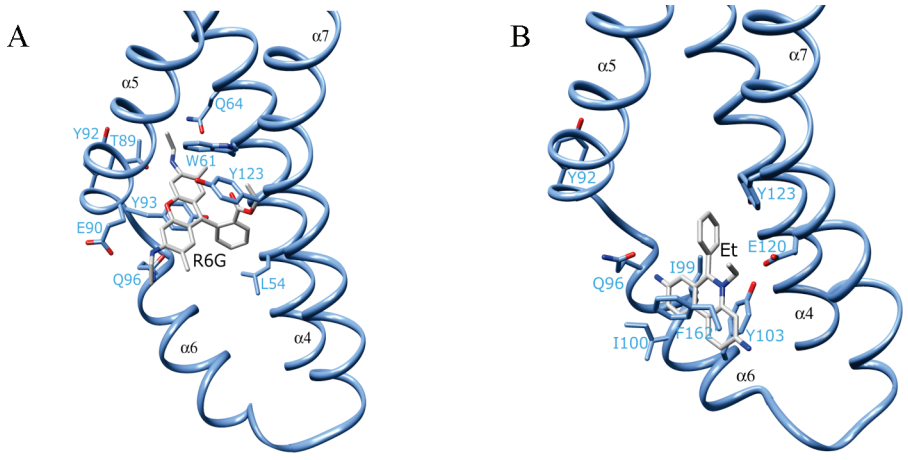

FIGURE 1: QacR ligand binding pocket bound to (A) rhodamine 6G (R6G) and (B) ethidium (Et). In addition, the tyrosine at position 92 (Y92) in the induction switch region is shown. Ligands are shown as sticks, and nitrogen and oxygen atoms are colored dark blue and red, respectively. Helices containing ligand interacting residues are labeled in black. This figure was generated using Chimera version 1.24 (*47*) and PDB entries 1JUS and 1JTY (*6*).

Specifically, ligand R6G binds further from the proposed ligand entrance of QacR than ligand Et and closer to the induction switch region (*6*). Here, the positively charged ethyl ammonium group of R6G is neutralized by Glu^{90}, with the compound stacking with Trp^{61} and Tyr^{93}, making hydrophobic contacts with Leu^{54} and Tyr^{123}, with further contacts mediated by Thr^{89} and Gln^{96} (*6*). In the Et subpocket, with the exception of contacts made with Gln^{96} and Tyr^{123}, Et makes unique contacts, interacting with key aromatic residues Tyr^{103} and $Phe^{162'}$ (where the prime indicates the second monomer in the dimer), in addition to making contacts with Ile^{99} and Ile^{100}, and is charge complemented by Glu^{120} (*6*). Our investigations of the functional contribution of Glu^{90} and Glu^{120} (unpublished data), and also of Glu^{57} and Glu^{58} which contact alternate QacR ligands (*20*), suggest that although the formal electrostatic contribution of these glutamate residues cannot be overlooked in conferring specificity to QacR−multidrug interactions, they alone do not appear to impart significant energy to ligand binding affinity. Thus, this responsibility has been duly attributed to aromatic, polar, and nonpolar residues that preside over the majority of QacR−ligand contacts. Indeed, these amino acids may be able to functionally compensate for glutamate residues in affording electrostatic complementation of cationic ligands. For example, in the complex of QacR with the bivalent ligand pentamidine, one of the two benzamidine moieties of pentamidine was complemented by Glu^{63}, whereas the other was complemented by $\pi-\pi$ and dipole charge interactions contributed from residues Ser^{86}, Tyr^{127}, Ala^{153}, and Ala^{157} (*8*). Similarly, following a substitution of Gln for Glu at position 58 in QacR, the ligand berberine was reoriented in the binding pocket such that the formal positive charge centered on the N1 atom was neutralized, not by Glu^{57} and Glu^{58} as observed in the wild-type (wt) protein, but by $\pi-\pi$ and dipole charge interactions contributed by residues Trp^{61}, Thr^{89}, and Tyr^{93} (*20*).

An abundance of aromatic and hydrophobic residues also appears to be characteristic of ligand binding pockets of many multidrug binding proteins, functionally proffered for the ligand binding capabilities of the transporters P-glycoprotein (*5*, *21*−*23*), EmrE (*24*−*27*), and QacA (*28*−*30*). Structural analyses of the multidrug binding transcriptional regulators BmrR (*12*), EthR (*31*, *32*), TtgR (*13*), and LmrR (*14*) have also identified a large number of hydrophobic and aromatic residues that contribute to protein−ligand contacts. In fact, as reviewed by Neyfakh (*33*) and Langton et al. (*34*), the involvement of such residues and their inability to form hydrogen bonds with what are generally hydrophobic cations are believed to be crucial to providing flexibility and, thus, broad specificity to intermolecular multidrug contacts mediated by a single protein. Polar residues have also been proposed to confer flexibility to ligand binding, permitting multisite binding of the ligand SR12813 to the human nuclear receptor PXR (*35*) and conceivably enabling the multidrug binding used by Sav1866, with the structure of this *Staphylococcus aureus* transport protein revealing a large cavity lined with a plethora of polar residues (*36*).

To comprehensively assess the functional significance of such residues in the QacR ligand binding pocket, this study involved the systematic targeting of key residues Tyr^{92} and Tyr^{93} in the induction switch and residues Leu^{54}, Trp^{61}, Gln^{64}, Thr^{89}, Gln^{96}, and Tyr^{123} in the QacR R6G subpocket by site-directed mutagenesis. The binding affinity of these QacR mutants for R6G and Et was assessed in vitro, and their repression and induction capabilities in the presence of these ligands were also examined in *S. aureus*.

MATERIALS AND METHODS

Bacterial Strains and Growth Conditions. All cloning and overexpression procedures performed in *Escherichia coli* utilized strain DH5α (*37*) and strain RN4220 *norA::erm* (SAK1759) (*38*) when in *S. aureus*. All strains were cultured at 37 °C in Luria-Bertani broth or agar (*37*) containing, where appropriate, 100 μg/mL ampicillin for *E. coli* or 20 μg/mL erythromycin and 10 μg/mL chloramphenicol for *S. aureus*. *E. coli* was transformed by standard procedures (*37*) and *S. aureus* by electroporation as described previously (*39*), employing a pulse of 1.3 kV.

DNA Isolation and Manipulations. The Quantum Prep plasmid miniprep kit (Bio-Rad) and small-scale alkaline lysis procedure (*40*) were employed in isolating plasmid DNA from *E. coli* and *S. aureus*, respectively. Restriction enzymes, T4 DNA ligase, calf intestinal alkaline phosphatase, and Taq DNA polymerase (all from New England Biolabs) were each used according to the manufacturer's instructions. Oligonucleotides were purchased from GeneWorks. PCR products were purified with the Wizard PCR Prep kit (Promega), and DNA fragments

were isolated from agarose gels using the GFX PCR and gel band purification kit (Amersham Biosciences).

Construction of QacR Mutants. QacR mutants were obtained by generating PCR-derived fragments encompassing the residue(s) to be mutated and replacing the wt sequence. This was achieved by subcloning into the *blaZ* reporter gene vector pSK5645 (*41*) and the pTTQ18-based *qacR* clone pSK5676 (*42*), which has a six-histidine tag incorporated at the QacR C-terminus. Automated DNA sequencing, performed at the Australian Genome Research Facility (Brisbane, Australia), was employed to verify the presence of the desired mutations and the absence of spurious mutations that may have been introduced during PCR.

Protein Purification. Mutant and wt QacR proteins were overexpressed from cells carrying plasmid derivatives of pSK5676, purified by Ni^{2+}-NTA metal chelate affinity chromatography (Invitrogen ProBond resin), and dialyzed against buffer A [1 M NaCl, 20 mM Tris-HCl, and 5% (v/v) glycerol (pH 7.5)] as previously described (*42*). The purified proteins were more than 99% pure as estimated from Coomassie-stained SDS−PAGE gels, and their concentrations were determined using the Coomassie plus protein assay reagent (Pierce).

Tryptophan Fluorescence Measurements. Fluorescence intensity measurements of QacR proteins were performed and K_d values calculated as described previously (*20*).

Western Analysis. Whole cell lysates of *S. aureus* strain SAK1759 (*38*) containing the desired plasmid were separated by SDS−12.5% PAGE and transferred to PVDF membrane. QacR was detected immunologically using a 1:1500 dilution of a rabbit polyclonal QacR antibody (*18*), and the secondary antibody was detected using the Immobilon Western chemiluminescent HRP substrate (Millipore) as described by the manufacturer. Blots were scanned with a ChemiDoc (Bio-Rad), and images were visualized and analyzed using Quantity One (Bio-Rad).

β-Lactamase Reporter Gene Assays. A stationary-phase culture of *S. aureus* strain SAK1759 (*38*) containing pSK5645 (*41*), or plasmids encoding wt or mutant QacR derivatives, was subcultured and grown to an OD_{600} of 0.6. Aliquots were then grown for a further 1.5 h in the presence or absence of inducing compounds, after which OD_{600} was measured and cells were collected by centrifugation. R6G and Et were employed at concentrations of 0.19 and 0.95 μM, and 7.71 and 17.09 μM, respectively. Cells were washed with cold 50 mM NaH_2PO_4, before being resuspended in an appropriate volume of the same buffer so that all treatments had a final OD_{600} of 13.5. β-Lactamase activities of washed whole cells were determined using the chromogenic substrate nitrocefin (Oxoid) as described previously (*43*) and are presented such that 1 unit corresponds to 1 μM nitrocefin hydrolyzed min^{-1} (μg of total cellular protein)$^{-1}$ at 37 °C. Results represent the average of at least two experiments.

RESULTS

Impact of QacR Mutations on Ligand Binding Affinity in Vitro. The ligand binding affinities of the wt and mutant QacR proteins for R6G and Et were determined by fluorescence quenching of intrinsic tryptophan residues. Of the three tryptophan residues that are present in QacR, only Trp^{61} resides in the ligand binding pocket (*6*). Therefore, ligand binding affinities of the QacR mutant Trp^{61}Ala, where tryptophan at position 61 has been replaced with alanine, and also of the double QacR mutant Trp^{61}Ala/Tyr^{93}Phe could not be assessed by this method. The binding affinity of QacR wt protein with Et and R6G was determined to be 0.5 ± 0.09 and 0.1 ± 0.01 μM, respectively. Binding affinities of the remaining mutants are shown in Figure 2 relative to wt QacR according to the term K_d^{mut-1}/K_d^{wt-1} (*44*), such that values below 1 represent a decrease in binding affinity and those above 1 an increase in binding affinity.

Substitution of aromatic, polar, and nonpolar QacR residues that interact with R6G and the proximally located Tyr^{92} (*6*)

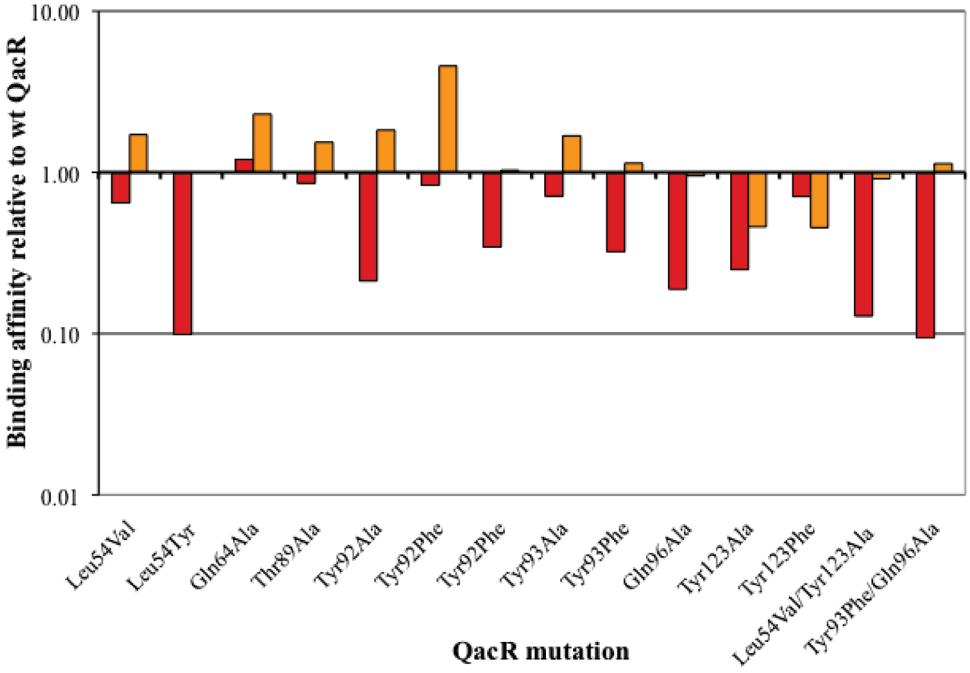

FIGURE 2: Effect of single and multiple substitutions of residues in the rhodamine 6G subpocket on the affinity of QacR for rhodamine 6G (red columns) and ethidium (orange columns). Each K_d value represents an average of three separate experiments with obtained values differing by no more than 7%. Binding affinities of mutants are shown relative to wt QacR according to the term K_d^{mut-1}/K_d^{wt-1} (*44*), such that values below 1 represent a decrease in binding affinity and those above 1 an increase in binding affinity.

Table 1: Effect of Substituting Key Aromatic, Polar, and Nonpolar Residues on QacR-Mediated Repression and Substrate-Induced Derepression in *S. aureus*

		R6G			Et		
QacR mutation	basal induction	intermediate induction[a]	maximum induction[a]	*x*-fold increase[b]	intermediate induction[a]	maximum induction[a]	*x*-fold increase[b]
wt	0.07 ± 0.01	0.22 ± 0.02	0.25 ± 0.01	3.6	0.12 ± 0.01	0.14 ± 0.00	2.0
$Leu^{54}Val$	0.10 ± 0.01	0.18 ± 0.02	0.24 ± 0.01	2.4	0.07 ± 0.00	0.09 ± 0.02	0.9
$Leu^{54}Tyr$	0.17 ± 0.01	0.13 ± 0.01	0.16 ± 0.03	0.9	0.20 ± 0.01	0.19 ± 0.01	1.1
$Trp^{61}Ala$	0.14 ± 0.00	0.23 ± 0.01	0.21 ± 0.01	1.5	0.19 ± 0.03	0.18 ± 0.01	1.3
$Gln^{64}Ala$	0.11 ± 0.00	0.18 ± 0.00	0.32 ± 0.00	2.9	0.18 ± 0.01	0.22 ± 0.00	2.0
$Thr^{89}Ala$	0.18 ± 0.00	0.22 ± 0.02	0.20 ± 0.01	1.1	0.25 ± 0.01	0.22 ± 0.03	1.4
$Tyr^{92}Ala$	0.03 ± 0.01	0.15 ± 0.01	0.20 ± 0.01	6.7	0.06 ± 0.01	0.08 ± 0.02	2.7
$Tyr^{92}Phe$	0.09 ± 0.02	0.26 ± 0.03	0.27 ± 0.03	3.0	0.30 ± 0.01	0.32 ± 0.03	3.6
$Tyr^{92}Pro$	0.26 ± 0.00	0.25 ± 0.00	0.30 ± 0.03	1.2	0.26 ± 0.01	0.20 ± 0.02	1.0
$Tyr^{93}Ala$	0.21 ± 0.00	0.24 ± 0.02	0.27 ± 0.01	1.3	0.23 ± 0.04	0.22 ± 0.04	1.1
$Tyr^{93}Phe$	0.07 ± 0.02	0.11 ± 0.01	0.18 ± 0.01	2.6	0.05 ± 0.01	0.08 ± 0.00	1.1
$Gln^{96}Ala$	0.12 ± 0.03	0.17 ± 0.00	0.22 ± 0.01	1.8	0.14 ± 0.01	0.16 ± 0.01	1.3
$Tyr^{123}Ala$	0.04 ± 0.01	0.08 ± 0.01	0.19 ± 0.02	4.8	0.05 ± 0.01	0.04 ± 0.01	1.0
$Tyr^{123}Phe$	0.07 ± 0.00	0.26 ± 0.01	0.25 ± 0.04	3.6	0.09 ± 0.02	0.08 ± 0.00	1.1
$Trp^{61}Ala/Tyr^{93}Phe$	0.10 ± 0.00	0.15 ± 0.02	0.21 ± 0.02	2.1	0.11 ± 0.01	0.15 ± 0.01	2.1
$Leu^{54}Val/Tyr^{123}Ala$	0.03 ± 0.00	0.06 ± 0.00	0.12 ± 0.01	4.0	0.03 ± 0.02	0.05 ± 0.00	1.7
$Tyr^{93}Phe/Gln^{96}Ala$	0.12 ± 0.00	0.13 ± 0.01	0.20 ± 0.03	1.7	0.13 ± 0.01	0.09 ± 0.03	0.8

[a]The concentrations of the QacR ligands required for intermediate and maximal induction of wt QacR were 0.19 and 0.95 μM, respectively, for rhodamine 6G (R6G) and 7.71 and 17.09 μM, respectively, for ethidium (Et). These concentrations were employed for induction with all QacR mutants. [b]The *x*-fold increase was calculated from the value for maximum induction relative to the basal induction value, the latter determined in the absence of inducing compound.

elicited a decrease, albeit generally moderate, in the binding affinity of QacR for this ligand (Figure 2). Specifically, the QacR mutant proteins $Leu^{54}Val$, $Gln^{64}Ala$, $Thr^{89}Ala$, $Tyr^{92}Phe$, $Tyr^{92}Pro$, $Tyr^{92}Ala$, $Tyr^{93}Phe$, $Tyr^{123}Ala$, and $Tyr^{123}Phe$ exhibited R6G binding affinity within 4-fold of that of wt QacR (Figure 2). Notably, despite the lack of a direct ligand interaction in the wt QacR−R6G complex (*6*), the alanine substitution of induction switch residue Tyr^{92} had a greater impact than that of the phenylalanine substitution [4.7-fold vs a 1.2-fold decrease, respectively (Figure 2)]. Marked decreases in binding affinity were observed for the QacR mutants $Leu^{54}Tyr$ and $Gln^{96}Ala$ which displayed 10.1- and 5.3-fold decreases in R6G affinity, respectively, with the double substitutions $Leu^{54}Val/Tyr^{123}Ala$ and $Tyr^{93}Phe/Gln^{64}Ala$ also displaying dramatic decreases of 7.8- and 10.6-fold, respectively (Figure 2).

Consistent with the absence of a direct interaction with Et, the replacements of Leu^{54}, Gln^{64}, and Thr^{89}, and also of Tyr^{92} and Tyr^{93}, did not dramatically alter the affinity of QacR for this ligand, with the most significant change observed for QacR $Tyr^{92}Phe$ showing a 4.6-fold increase in Et affinity (Figure 2). However, this was also true of the single and multiple substitutions involving Gln^{96} and Tyr^{123}, which are shared between the Et and R6G subpockets (*6*), with the maximum decrease in binding affinity following the mutation of these residues being in the order of 2.2-fold (Figure 2).

Repression and Induction Capabilities of the QacR Mutants in S. aureus. The ability of the wt and mutant QacR proteins to bind to IR1 operator DNA and subsequently dissociate in the presence of the inducing compounds Et and R6G, thereby leading to derepression of the divergently transcribed *qacA* determinant, was analyzed using gene reporter assays. These assays utilized pSK5645 (*41*), a plasmid in which P_{qacA} directs transcription of *blaZ*, the enzyme activity of which is monitored colorimetrically; studies were conducted in *S. aureus* strain RN4220 *norA::erm* (SAK1759) (*38*). This strain was employed to prevent the masking of inducers by the chromosomally encoded multidrug exporter NorA that shares substrates in common with the QacA/QacR system (*42*). The *blaZ* reporter gene vector pSK5645 (*41*), and derivatives encoding wt and mutant QacR proteins, were electroporated into this strain, and expression levels of mutant proteins relative to wt QacR were assessed by immunological detection. With the exception of the four QacR derivatives $Leu^{54}Tyr$, $Trp^{61}Ala$, $Tyr^{92}Pro$, and $Trp^{61}Ala/Tyr^{93}Phe$, the expression levels of the mutant proteins were no less than 40% and were typically at, or above, 80% of wt QacR levels (data not shown).

β-Lactamase activity detected from SAK1759 harboring pSK5645 was minimal and was used to normalize the data. In the absence of inducing compounds, the basal levels of β-lactamase activity observed in strains expressing QacR mutants $Tyr^{92}Phe$, $Tyr^{93}Phe$, $Tyr^{123}Phe$, and $Trp^{61}Ala/Tyr^{93}Phe$ were comparable to that of wt QacR. However, indicative of impaired repression capabilities, the basal level of β-lactamase activity was increased between 1.7- and 3.7-fold in the presence of QacR mutants $Tyr^{93}Phe/Gln^{96}Ala$, $Trp^{61}Ala$, $Leu^{54}Tyr$, $Tyr^{93}Ala$, and $Tyr^{92}Pro$ (Table 1). Conversely, QacR mutants $Tyr^{92}Ala$, $Tyr^{123}Ala$, and $Leu^{54}Val/Tyr^{123}Ala$ exhibited improved repression capabilities, displaying ~2-fold decreases in the basal level of β-lactamase activity relative to that observed in the presence of wt QacR (Table 1). Thus, although the numerical fold induction of these mutants was significantly elevated, the maximal induction values were significantly lower than that of wt QacR (Table 1).

The inducing compounds R6G and Et were employed at concentrations that afforded intermediate and maximum induction from P_{qacA}-*blaZ* in the presence of wt QacR. The majority of the QacR mutants examined displayed induction in the presence of R6G, and indeed, QacR mutants $Leu^{54}Val$, $Trp^{61}Ala$, $Tyr^{92}Phe$, $Gln^{96}Ala$, and $Tyr^{123}Phe$ collectively exhibited induction profiles and maximal induction values comparable to those of wt QacR in the presence of R6G (Table 1). Notably, however, little to no induction was observed in the presence of R6G or Et for QacR mutants $Leu^{54}Tyr$, $Thr^{89}Ala$, $Tyr^{92}Pro$, and $Tyr^{93}Ala$, all of which exhibited high basal levels of β-lactamase activity that, for the most part, were comparable to the maximal level of

activity observed for wt QacR in the presence of R6G (Table 1). Similarly, the QacR mutants Tyr^{92}Ala, Tyr^{93}Phe, Tyr^{123}Ala, Leu^{54}Val/Tyr^{123}Ala, Trp^{61}Ala/Tyr^{93}Phe, and Tyr^{93}Phe/Gln^{96}Ala also exhibited impaired induction with submaximal induction levels 1.5−3.75-fold lower than that of wt QacR at the intermediate R6G concentration (Table 1).

β-Lactamase activity was increased by 2.7- or 3.6-fold by Et in the presence of QacR Tyr^{92}Ala or Tyr^{92}Phe, respectively, an increase that was significantly higher than the 2.0-fold increase observed in the presence of wt QacR (Table 1). Intriguingly, although QacR Trp^{61}Ala and QacR double mutant Trp^{61}Ala/Tyr^{93}Phe displayed an induction profile comparable to that of wt QacR in the presence of Et, QacR mutants Leu^{54}Val, Tyr^{123}Ala, Tyr^{123}Phe, Leu^{54}Val/Tyr^{123}Ala, Tyr^{93}Phe, and Tyr^{93}Phe/Gln^{96}Ala were not induced by this ligand in vivo, and induction of the QacR Gln^{96}Ala variant was impaired (Table 1).

DISCUSSION

Comparison of the previously determined affinity of wt QacR for IR1 operator DNA (5.7 nM) (*7*) and for a diverse range of ligands ($K_d \sim 10^6$ M^{-1}) (*42*) suggests that as opposed to affinity, the conformational changes associated with ligand binding are crucial to the induction process. However, the binding affinity and induction capabilities of QacR in the presence of Et and R6G, two ligands chosen as representatives as they bind to the two extreme regions of the ligand binding pocket, were found in this study to be neither abolished nor dramatically altered by the phenylalanine or alanine substitutions of Tyr^{92} (Figure 2). This residue represents the only Ramachandran outlier in the ligand-free dimer and reportedly facilitates the key coil−helix transition required for the induction mechanism and expansion of the drug binding pocket (*6*). Indeed, the induction capabilities of these mutants in vivo using *S. aureus* corresponded well with the moderate changes in ligand binding affinities in vitro (Figure 2 and Table 1), suggesting that they were governed by affinity as opposed to having a general impact on the coil−helix mechanism and the transition of QacR to the ligand-bound conformation. Nevertheless, commensurate with a role in expanding the ligand binding pocket upon induction (*6*), Tyr^{92} does exert long-range effects on the specificity of ligand binding sites. Notably, the flexibility of the distally located Et subpocket was augmented by the Tyr^{92}Phe substitution, increasing Et affinity and induction capacity in *S. aureus* by presumably expanding the binding site preferences available for this ligand (Figure 2 and Table 1).

In a further attempt to hinder the QacR coil−helix transition and the subsequent creation of the multidrug binding pocket, Tyr^{92} was substituted with proline, a residue that is known to disrupt the formation of α-helices (*45*). However, this had an only moderate impact on the ability of QacR to bind to the representative ligands (Figure 2). One possible explanation for this unexpected result was conveyed by the protein stability and repression capabilities of this mutant which were significantly impaired in *S. aureus* relative to wt QacR (Table 1), with the misfolding of the QacR Tyr^{92}Pro protein perhaps permanently assigning QacR to the ligand-bound conformation rather than the uninduced conformation intended.

The structure of QacR in complex with multiple ligands also suggests a subsidiary role for Tyr^{93} in the induction mechanism, proposed to act in conjunction with Tyr^{92} to stabilize the hydrophobic core of the protein in the absence of ligand and similarly expelled in the coil−helix transition (*6*). In contrast to QacR mutants Tyr^{92}Ala, Tyr^{92}Phe, and Tyr^{93}Phe, the protein stability and repression capabilities of QacR Tyr^{93}Ala in *S. aureus* were significantly impaired (Table 1), suggesting that a nonaromatic residue at position 93 does significantly disrupt the formation of the tertiary QacR structure. Thus, as opposed to both Tyr^{92} and Tyr^{93} acting as ligand surrogates, this study suggests that an aromatic residue at position 93 is sufficient and, indeed, dominates this role. In fact, QacR Tyr^{92}Ala exhibited increased protein stability relative to wt QacR, which corresponded with improved repression capabilities in *S. aureus* (Table 1). Although it appeared that this substitution benefited QacR, these so-called repressive deficiencies in the wt protein may be imperative to the success of the *qacA*−*qacR* multidrug resistance locus, permitting a basal level of *qacA* transcription that, as suggested by Grkovic et al. (*16*), affords protection of *S. aureus* against substrates of the QacA pump that are not efficient inducers of QacR.

Unexpectedly, the substitution of residues that line the R6G subpocket identified amino acids that are key to the induction mechanism preceding the coil−helix transition. QacR mutants Leu^{54}Val, Tyr^{123}Ala, Tyr^{93}Phe, and to a lesser extent Gln^{96}Ala and those QacR mutants containing combinations of multiple substitutions of these residues, Leu^{54}Val/Tyr^{123}Ala and Tyr^{93}Phe/Gln^{96}Ala, although capable of induction in the presence of R6G, were unable to be induced by Et in *S. aureus* (Table 1) despite retaining high affinity for this ligand in vitro (Figure 2). This may be attributable to the fact that although R6G binding directly involves and, thus, directly communicates with amino acids in the induction switch region, these substitutions may hinder the signal conferred to trigger the induction switch from the distally located Et subpocket. Consistent with this notion, Leu^{54}, Gln^{96}, and Tyr^{123} denote the boundary between the Et and R6G subpockets (Figure 3), with Et directly contacting Gln^{96} and Tyr^{123} when in complex with wt QacR (see Figure 1B) (*6*).

The ability of QacR to bind to R6G and also to Et was largely unaffected by individual substitutions of Thr^{89} or Tyr^{123} which from structural analyses are directly involved in R6G binding (Figure 1) (*6*) and were typically associated with moderate changes in both affinity in vitro and induction capabilities in *S. aureus* (Figure 2 and Table 1). This correlates with the fact that each of these residues affords only one of many QacR−R6G contacts that may individually and predominantly contribute low-energy van der Waals and stacking interactions. This premise was similarly asserted for the multidrug binding repressor BmrR, where alanine substitutions of aromatic and hydrophobic residues that, as evidenced by structural analyses, interact with the ligand TPP conferred only moderate effects on ligand affinities (*44*). Furthermore, intrinsic to the voluminous and highly flexible nature of the QacR multidrug binding pocket, the reorientation of ligands may be permitted, and subsequently, residue substitution may be tolerated by an abundance of functionally equivalent residues either within the immediate vicinity of a given ligand binding site or in distinct binding sites that employ an alternative complement of like residues (*20*). The multiple binding sites of PXR for a single ligand, SR12813, which are governed by aromatic and polar residues, provide quintessential testament to this premise (*35*). Moreover, the recent determination of the structure of the mouse multidrug transporter P-glycoprotein in combination with two inhibitory molecules revealed the importance of having a multitude of hydrophobic and aromatic residues forming the drug binding pocket. Like the

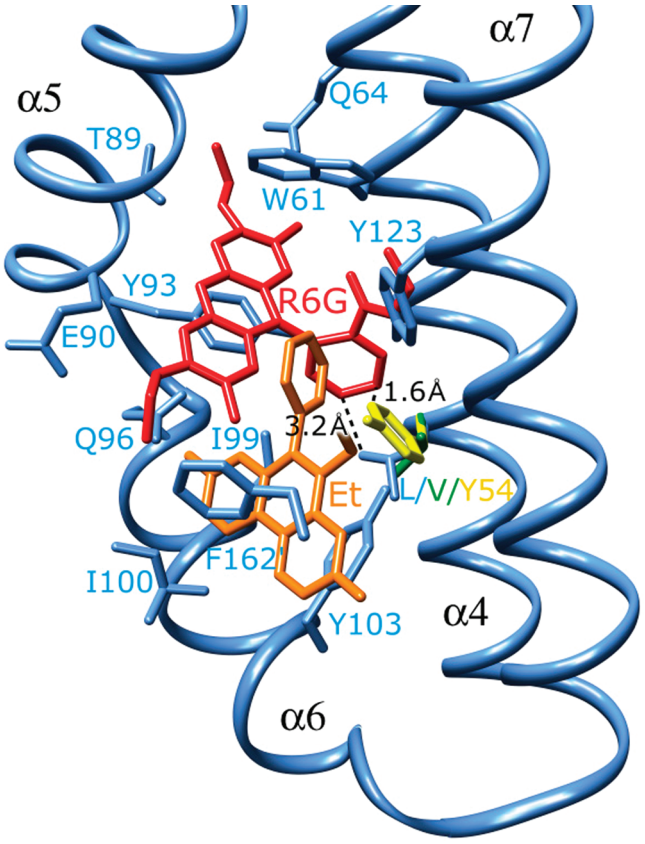

FIGURE 3: Superimposition of QacR rhodamine 6G (R6G) and ethidium (Et) binding sites and the predicted impact of the L54V and L54Y substitutions. R6G and Et are shown as red and orange sticks, respectively. Helices containing ligand interacting residues are labeled in black, and the predicted positions of the side chains of L54V and L54Y are colored green and yellow, respectively. The distances between R6G and L54 and Y54 are labeled and shown as dashed lines. This figure was generated using Chimera version 1.24 (*47*) and PDB entries 1JUS, 1JTY (*6*), and 1JUS containing the L54V and L54Y substitutions, which were generated using PyMOL (*46*).

drug binding mechanism of QacR, the two peptide ligands of P-glycoprotein bind within a large binding pocket, interacting with distinct subsets of residues, some of which are specific for each molecule and some in common (*5*).

Nevertheless, the presence of a small hydrophobic side chain at Leu^{54} and the integrity of Trp^{61} and Thr^{89} were crucial for the stability of QacR in *S. aureus* (Table 1). This may reflect the position of Leu^{54} and Trp^{61} in α-helix 4, which is involved in the repositioning of the DNA binding domain and Thr^{89} in the induction switch (*6*) with residues within these α-helices optimally enlisted for their ability to stabilize the tertiary protein structure while conferring the flexibility necessary for the regulatory function of QacR. In addition, the single Leu^{54}Tyr and Gln^{96}Ala substitutions and the substitutions that simultaneously targeted multiple R6G contacts, viz., Leu^{54}Val/Tyr^{123}Ala and Tyr^{93}Phe/Gln^{96}Ala, maintained Et affinity yet significantly diminished R6G binding affinity (Figure 2), indicating that there are structural and/or energetic limits to the versatility of QacR−R6G binding. These changes in affinity were reflected in impaired induction capabilities in the presence of R6G in *S. aureus* (Table 1).

High-resolution structures of these functionally altered QacR mutants in complex with R6G have yet to be resolved. Nevertheless, it is likely that these substitutions have successfully identified residues that collectively contribute important contacts with this ligand, either abolishing energetically important contacts or precluding the preferential access of R6G to this high-affinity site. Indeed, one backbone-dependent orientation of the QacR Leu^{54}Tyr side chain afforded by protein modeling using PyMOL (*46*) would conceivably permit access of Et to its subpocket, which lies adjacent to the entrance of the QacR ligand binding pocket, yet constrain access and clash with R6G in the wt QacR−R6G complex (Figure 3).

The impacts of the single substitutions Leu^{54}Val and Tyr^{123}Ala, and Tyr^{93}Phe and Gln^{96}Ala, were additive in the Leu^{54}Val/Tyr^{123}Ala and Tyr^{93}Phe/Gln^{96}Ala mutants with regard to the binding affinity of QacR for R6G (Figure 2). The combined impact of the Leu^{54}Val/Tyr^{123}Ala substitution, collectively targeting residues located on the same side of this binding pocket, may effectively destabilize the QacR−R6G interaction. With regard to the Tyr^{93}Phe/Gln^{96}Ala double substitution, rather than obstructing the binding site which was proposed for Leu^{54}Tyr, Gln^{96}Ala may not only eliminate the polarity of the side chain at this position but also completely abolish the interaction of residue 96 with R6G. In addition, since the alanine substitution of Tyr^{93} did not affect R6G binding affinity (Figure 2), it would appear that although an aromatic residue is not required at this position for R6G binding, the removal of the hydroxyl group, which otherwise forms a salt bridge with Glu^{57}, may free this side chain to rotate to a position such that it hinders R6G binding or mediates a less favorable stacking interaction.

In conclusion, this study demonstrates that despite the functional plasticity afforded by a plethora of relatively weak QacR−ligand contacts there are structural limitations to the ligand binding capabilities of QacR, not the least of which are residues that delineate the R6G−Et subpocket interface and communicate distal ligand binding to confer QacR induction.

ACKNOWLEDGMENT

We thank Dr. Slade Jensen (University of Sydney) for assistance with the tryptophan fluorescence measurements and Dr. Kate Newberry (M. D. Anderson Cancer Center, University of Texas, Houston, TX) for useful discussions.

REFERENCES

1. Paulsen, I. T., Brown, M. H., and Skurray, R. A. (1996) Proton-dependent multidrug efflux systems. *Microbiol. Rev. 60*, 575–608.
2. Higgins, C. F. (2007) Multiple molecular mechanisms for multidrug resistance transporters. *Nature 446*, 749–757.
3. Murakami, S., Nakashima, R., Yamashita, E., Matsumoto, T., and Yamaguchi, A. (2006) Crystal structures of a multidrug transporter reveal a functionally rotating mechanism. *Nature 443*, 173–179.
4. Dawson, R. J., and Locher, K. P. (2006) Structure of a bacterial multidrug ABC transporter. *Nature 443*, 180–185.
5. Aller, S. G., Yu, J., Ward, A., Weng, Y., Chittaboina, S., Zhuo, R., Harrell, P. M., Trinh, Y. T., Zhang, Q., Urbatsch, I. L., and Chang, G. (2009) Structure of P-glycoprotein reveals a molecular basis for poly-specific drug binding. *Science 323*, 1718–1722.
6. Schumacher, M. A., Miller, M. C., Grkovic, S., Brown, M. H., Skurray, R. A., and Brennan, R. G. (2001) Structural mechanisms of QacR induction and multidrug recognition. *Science 294*, 2158–2163.
7. Schumacher, M. A., Miller, M. C., and Brennan, R. G. (2004) Structural mechanism of the simultaneous binding of two drugs to a multidrug-binding protein. *EMBO J. 23*, 2923–2930.
8. Murray, D. S., Schumacher, M. A., and Brennan, R. G. (2004) Crystal structures of QacR-diamidine complexes reveal additional multidrug-binding modes and a novel mechanism of drug charge neutralization. *J. Biol. Chem. 279*, 14365–14371.
9. Brooks, B. E., Piro, K. M., and Brennan, R. G. (2007) Multidrug-binding transcription factor QacR binds the bivalent aromatic

diamidines DB75 and DB359 in multiple positions. *J. Am. Chem. Soc. 129*, 8389–8395.
10. Newberry, K. J., Huffman, J. L., Miller, M. C., Vazquez-Laslop, N., Neyfakh, A. A., and Brennan, R. G. (2008) Structures of BmrR-drug complexes reveal a rigid multidrug binding pocket and transcription activation through tyrosine expulsion. *J. Biol. Chem. 283*, 26795–26804.
11. Heldwein, E. E., and Brennan, R. G. (2001) Crystal structure of the transcription activator BmrR bound to DNA and a drug. *Nature 409*, 378–382.
12. Zheleznova, E. E., Markham, P. N., Neyfakh, A. A., and Brennan, R. G. (1999) Structural basis of multidrug recognition by BmrR, a transcriptional activator of a multidrug transporter. *Cell 96*, 353–362.
13. Alguel, Y., Meng, C., Teran, W., Krell, T., Ramos, J. L., Gallegos, M. T., and Zhang, X. (2007) Crystal structures of multidrug binding protein TtgR in complex with antibiotics and plant antimicrobials. *J. Mol. Biol. 369*, 829–840.
14. Madoori, P. K., Agustiandari, H., Driessen, A. J., and Thunnissen, A. M. (2009) Structure of the transcriptional regulator LmrR and its mechanism of multidrug recognition. *EMBO J. 28*, 156–166.
15. Ramos, J. L., Martinez-Bueno, M., Molina-Henares, A. J., Teran, W., Watanabe, K., Zhang, X., Gallegos, M. T., Brennan, R., and Tobes, R. (2005) The TetR family of transcriptional repressors. *Microbiol. Mol. Biol. Rev. 69*, 326–356.
16. Grkovic, S., Brown, M. H., and Skurray, R. A. (2002) Regulation of bacterial drug export systems. *Microbiol. Mol. Biol. Rev. 66*, 671–701.
17. Rouch, D. A., Cram, D. S., DiBerardino, D., Littlejohn, T. G., and Skurray, R. A. (1990) Efflux-mediated antiseptic resistance gene *qacA* from *Staphylococcus aureus*: Common ancestry with tetracycline- and sugar-transport proteins. *Mol. Microbiol. 4*, 2051–2062.
18. Grkovic, S., Brown, M. H., Schumacher, M. A., Brennan, R. G., and Skurray, R. A. (2001) The staphylococcal QacR multidrug regulator binds a correctly spaced operator as a pair of dimers. *J. Bacteriol. 183*, 7102–7109.
19. Schumacher, M. A., Miller, M. C., Grkovic, S., Brown, M. H., Skurray, R. A., and Brennan, R. G. (2002) Structural basis for cooperative DNA binding by two dimers of the multidrug binding protein QacR. *EMBO J. 21*, 1210–1218.
20. Peters, K. M., Schuman, J. T., Skurray, R. A., Brown, M. H., Brennan, R. G., and Schumacher, M. A. (2008) QacR-cation recognition is mediated by a redundancy of residues capable of charge neutralization. *Biochemistry 47*, 8122–8129.
21. Pawagi, A. B., Wang, J., Silverman, M., Reithmeier, R. A. F., and Deber, C. M. (1994) Transmembrane aromatic amino acid distribution in P-glycoprotein: A functional role in broad substrate specificity. *J. Mol. Biol. 235*, 554–564.
22. Loo, T. W., and Clarke, D. M. (1993) Functional consequences of phenylalanine mutations in the predicted transmembrane domain of P-glycoprotein. *J. Biol. Chem. 268*, 19965–19972.
23. Kwan, T., Loughrey, H., Brault, M., Gruenheid, S., Urbatsch, I. L., Senior, A. E., and Gros, P. (2000) Functional analysis of a tryptophan-less P-glycoprotein: A tool for tryptophan insertion and fluorescence spectroscopy. *Mol. Pharmacol. 58*, 37–47.
24. Rotem, D., Steiner-Mordoch, S., and Schuldiner, S. (2006) Identification of tyrosine residues critical for the function of an ion-coupled multidrug transporter. *J. Biol. Chem. 281*, 18715–18722.
25. Schuldiner, S., Granot, D., Steiner, S., Ninio, S., Rotem, D., Soskin, M., and Yerushalmi, H. (2001) Precious things come in little packages. *J. Mol. Microbiol. Biotechnol. 3*, 155–162.
26. Sharoni, M., Steiner-Mordoch, S., and Schuldiner, S. (2005) Exploring the binding domain of EmrE, the smallest multidrug transporter. *J. Biol. Chem. 280*, 32849–32855.
27. Elbaz, Y., Tayer, N., Steinfels, E., Steiner-Mordoch, S., and Schuldiner, S. (2005) Substrate-induced tryptophan fluorescence changes in EmrE, the smallest ion-coupled multidrug transporter. *Biochemistry 44*, 7369–7377.
28. Brown, M. H., and Skurray, R. A. (2001) Staphylococcal multidrug efflux protein QacA. *J. Mol. Microbiol. Biotechnol. 3*, 163–170.
29. Xu, Z., O'Rourke, B. A., Skurray, R. A., and Brown, M. H. (2006) Role of transmembrane segment 10 in efflux mediated by the staphylococcal multidrug transport protein QacA. *J. Biol. Chem. 281*, 792–799.
30. Hassan, K. A., Souhani, T., Skurray, R. A., and Brown, M. H. (2008) Analysis of tryptophan residues in the staphylococcal multidrug transporter QacA reveals long-distance functional associations of residues on opposite sides of the membrane. *J. Bacteriol. 190*, 2441–2449.
31. Frènois, F., Engohang-Ndong, J., Locht, C., Baulard, A. R., and Villeret, V. (2004) Structure of EthR in a ligand bound conformation reveals therapeutic perspectives against tuberculosis. *Mol. Cell 16*, 301–307.
32. Dover, L. G., Corsino, P. E., Daniels, I. R., Cocklin, S. L., Tatituri, V., Besra, G. S., and Futterer, K. (2004) Crystal structure of the TetR/CamR family repressor *Mycobacterium tuberculosis* EthR implicated in ethionamide resistance. *J. Mol. Biol. 340*, 1095–1105.
33. Neyfakh, A. A. (2002) Mystery of multidrug transporters: The answer can be simple. *Mol. Microbiol. 44*, 1123–1130.
34. Langton, K. P., Henderson, P. J., and Herbert, R. B. (2005) Antibiotic resistance: Multidrug efflux proteins, a common transport mechanism? *Nat. Prod. Rep. 22*, 439–451.
35. Watkins, R. E., Wisely, G. B., Moore, L. B., Collins, J. L., Lambert, M. H., Williams, S. P., Willson, T. M., Kliewer, S. A., and Redinbo, M. R. (2001) The human nuclear xenobiotic receptor PXR: Structural determinants of directed promiscuity. *Science 292*, 2329–2333.
36. Dawson, R. J., and Locher, K. P. (2007) Structure of the multidrug ABC transporter Sav1866 from *Staphylococcus aureus* in complex with AMP-PNP. *FEBS Lett. 581*, 935–938.
37. Sambrook, J., Fritsch, E. F., and Maniatis, T. (1989) Molecular Cloning: A Laboratory Manual , 2nd ed., Cold Spring Harbor Laboratory Press, Plainview, NY.
38. Price, C. T., Kaatz, G. W., and Gustafson, J. E. (2002) The multidrug efflux pump NorA is not required for salicylate-induced reduction in drug accumulation by *Staphylococcus aureus*. *Int. J. Antimicrob. Agents 20*, 206–213.
39. Schenk, S., and Laddaga, R. A. (1992) Improved method for electroporation of *Staphylococcus aureus*. *FEMS Microbiol. Lett. 73*, 133–138.
40. Lyon, B. R., May, J. W., and Skurray, R. A. (1983) Analysis of plasmids in nosocomial strains of multiple-antibiotic-resistant *Staphylococcus aureus*. *Antimicrob. Agents Chemother. 23*, 817–826.
41. Grkovic, S., Brown, M. H., Hardie, K. M., Firth, N., and Skurray, R. A. (2003) Stable low-copy-number *Staphylococcus aureus* shuttle vectors. *Microbiology 149*, 785–794.
42. Grkovic, S., Hardie, K. M., Brown, M. H., and Skurray, R. A. (2003) Interactions of the QacR multidrug-binding protein with structurally diverse ligands: Implications for the evolution of the binding pocket. *Biochemistry 42*, 15226–15236.
43. Yoon, K. P., Misra, T. K., and Silver, S. (1991) Regulation of the *cadA* cadmium resistance determinant of *Staphylococcus aureus* plasmid pI258. *J. Bacteriol. 173*, 7643–7649.
44. Vázquez-Laslop, N., Markham, P. N., and Neyfakh, A. A. (1999) Mechanism of ligand recognition by BmrR, the multidrug-responding transcriptional regulator: Mutational analysis of the ligand-binding site. *Biochemistry 38*, 16925–16931.
45. Chou, P. Y., and Fasman, G. D. (1978) Prediction of the secondary structure of proteins from their amino acid sequence. *Adv. Enzymol. 47*, 45–148.
46. Delano, W. L. (2006) The PyMOL Molecular Graphics System, DeLano Scientific, Palo Alto, CA.
47. Pettersen, E. F., Goddard, T. D., Huang, C. C., Couch, G. S., Greenblatt, D. M., Meng, E. C., and Ferrin, T. E. (2004) UCSF Chimera: A visualization system for exploratory research and analysis. *J. Comput. Chem. 25*, 1605–1612.